nature immunology

Exosomes mediate the cell-to-cell transmission of IFN-α-induced antiviral activity

Jianhua Li[1], Kuancheng Liu[1], Yang Liu[1], Yan Xu[1], Fei Zhang[1], Huijuan Yang[1], Jiangxia Liu[1], Tingting Pan[1], Jieliang Chen[1], Min Wu[2], Xiaohui Zhou[3] & Zhenghong Yuan[1,2]

The cell-to-cell transmission of viral resistance is a potential mechanism for amplifying the interferon-induced antiviral response. In this study, we report that interferon-α (IFN-α) induced the transfer of resistance to hepatitis B virus (HBV) from nonpermissive liver nonparenchymal cells (LNPCs) to permissive hepatocytes via exosomes. Exosomes from IFN-α-treated LNPCs were rich in molecules with antiviral activity. Moreover, exosomes from LNPCs were internalized by hepatocytes, which mediated the intercellular transfer of antiviral molecules. Finally, we found that exosomes also contributed to the antiviral response of IFN-α to mouse hepatitis virus A59 and adenovirus in mice. Thus, we propose an antiviral mechanism of IFN-α activity that involves the induction and intercellular transfer of antiviral molecules via exosomes.

The intricate relationships among various viral and host factors determines whether viral clearance or persistence occurs. Type I interferons, mainly interferon-α (IFN-α) and IFN-β, serve an important role in controlling viral replication during the initial stages of infection[1]. Thus, type I interferons function as natural antiviral mechanisms and have various therapeutic applications[1,2]. After binding to the interferon receptor complex (IFNAR1-IFNAR2), IFN-α and IFN-β signal through a kinase of the Jak family to the signal-transduction-and-activator-of-transcription (STAT) pathway to initiate the transcription of interferon-stimulated genes (ISGs), which are under the control of interferon-stimulated response elements (ISREs)[1]. The expression products of those ISGs establish an antiviral state in the target cells[1]. However, viral proteins can target multiple steps in the IFN-α signaling cascade[3] and thus counteract the antiviral state in virus-infected cells. To amplify the efficiency of cellular antiviral activity, IFN-α induces the transfer of viral resistance from nonpermissive cells to cells that permit viral replication, via intercellular communication[4].

Exosomes are membrane vesicles with diameters of 40–100 nm that originate in the late endosomal compartment from the inward budding of endosomal membranes, which generates intracellular multivesicular bodies (MVBs)[5,6]. Pools of exosomes are packed in the MVBs and are released into the extracellular environment after the fusion of MVBs with the plasma membrane[5,6]. Those vesicles can 'horizontally' transfer functional protein, mRNA and microRNA (miRNA) to neighboring cells and thus serve as mediators of intercellular communication[7–12]. It is conceivable that the exosome-mediated intercellular transfer of functional molecules is a mechanism through which the interferon-induced antiviral response is amplified while the virus-mediated inhibition of ISG expression is bypassed in virus-infected cells. An ideal model system with which to address this hypothesis would be one in which the virus is unable to replicate in the cells that respond to IFN-α but does replicate in neighboring cells that are not responsive to IFN-α because of viral inhibition of the IFN-α signaling pathway[13].

Hepatitis B virus (HBV) belongs to the *Hepadnaviridae* family, which exclusively infects hepatocytes[14]. Approximately 400 million people are chronically infected with HBV worldwide[15]. IFN-α is now approved for the treatment of chronic infection with HBV and has a response rate of 30–40% (ref. 16). Paradoxically, IFN-α does not inhibit, or only modestly inhibits, HBV replication in human hepatocyte-derived cell lines[17,18]; this may be partially due to the blockade of IFN-α-induced signaling by the cytoplasmic retention and inactivation of STAT1 and STAT2 induced by viral proteins[19,20]. The liver's immune system is characterized mainly by innate immunity[21], and the organ is composed of both liver parenchymal cells (hepatocytes) and nonparenchymal cells. The liver nonparenchymal cells (LNPCs), which include Kupffer cells (the resident macrophages of the liver), liver sinusoidal endothelial cells (LSECs) and lymphocytes, account for approximately one third of the total liver cell population[22]. Here we investigated whether the IFN-α-induced antiviral response could be transmitted from LNPCs to HBV-infected hepatocytes via exosomes and thus restore the antiviral state in hepatocytes. We provide evidence that IFN-α induced the cell-to-cell transfer, via exosomes, of antiviral molecules directed against HBV both *in vitro* and *in vivo*.

RESULTS

Cell-to-cell transfer of IFN-α-induced viral resistance

To investigate whether LNPCs contribute to the antiviral activity of IFN-α against HBV, we individually cultured human macrophages

[1]Key Laboratory of Medical Molecular Virology, School of Basic Medical Sciences, Shanghai Medical College, Fudan University, Shanghai, China. [2]Research Unit, Shanghai Public Health Clinical Center, Fudan University, Shanghai, China. [3]Center of Laboratory Animals, Shanghai Public Health Clinical Center, Fudan University, Shanghai, China. Correspondence should be addressed to Z.Y. (zhyuan@shaphc.org).

Received 27 March; accepted 17 May; published online 7 July 2013; doi:10.1038/ni.2647

(THP-1 cells), a human LSEC line or HepG2 human hepatoma cells together with the HepG2 derivative HepG2.2.15 (in which HBV replicates) in a Transwell system (**Supplementary Fig. 1a**), to allow transfer of exosomes but preclude direct cell contact, and treated the cultures with IFN-α. We assessed the abundance of extracellular HBV virions and intracellular nucleocapsids by Southern blot analysis. HepG2.2.15 cells cultured with macrophages or LSECs had lower HBV production and DNA replication after treatment with IFN-α, but HepG2.2.15 cells cultured alone did not (**Fig. 1a**). Additionally, the antiviral activity of IFN-α depended on the number of macrophages or LSECs (**Supplementary Fig. 1b**). These findings indicated the involvement of LNPCs in the antiviral activity of IFN-α against HBV in HepG2.2.15 cells. In contrast, treatment of the cocultured HepG2 and HepG2.2.15 cells with IFN-α did not result in less HBV replication (**Fig. 1a**), which suggested that the IFN-α-induced antiviral activity was specific to the cell type.

To determine whether the IFN-α-induced Jak-STAT signaling pathway was required for the LNPC-mediated antiviral activity of IFN-α, we first examined the responses of HepG2 and HepG2.2.15 cells, macrophages and LSECs to IFN-α by monitoring ISRE activity and translocation of STAT1 to the nucleus. Consistent with published reports[20,23], the HepG2.2.15 cells were less sensitive to IFN-α than were the virus-free parental HepG2 cells (**Fig. 1b** and **Supplementary Fig. 1c**). Both the macrophages and LSECs responded robustly to IFN-α (**Fig. 1b** and **Supplementary Fig. 1c**).

Next, to block the Jak-STAT pathway, we knocked down STAT1 expression in each of the cell types (HepG2.2.15 cells, macrophages and LSECs), as demonstrated by the lower abundance of total and phosphorylated STAT1 (**Fig. 1c**) and diminished activity of the ISRE (**Supplementary Fig. 1d**). The suppression of STAT1 expression in HepG2.2.15 cells did not blunt the macrophage- or LSEC-mediated anti-HBV activity of IFN-α in the HepG2.2.15 cells (**Fig. 1d**,**e**). However, the antiviral effects of IFN-α were abrogated after knockdown of STAT1 in macrophages and LSECs (**Fig. 1d**,**e**). These results suggested that the IFN-α-induced suppression of HBV replication in HepG2.2.15 cells was due to cell-to-cell transmission of the antiviral response of the macrophages and LSECs with which they were cultured.

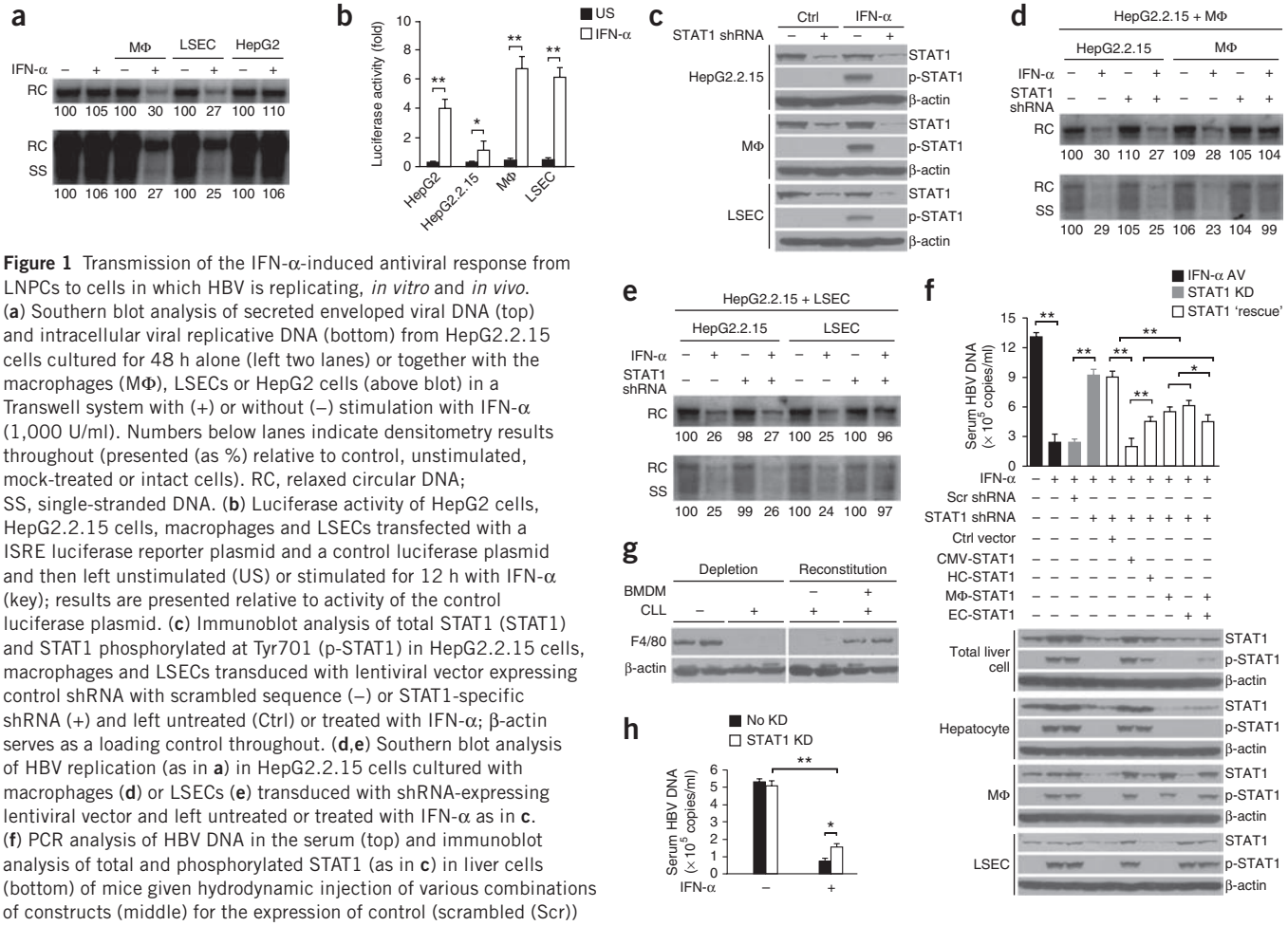

Figure 1 Transmission of the IFN-α-induced antiviral response from LNPCs to cells in which HBV is replicating, *in vitro* and *in vivo*. (**a**) Southern blot analysis of secreted enveloped viral DNA (top) and intracellular viral replicative DNA (bottom) from HepG2.2.15 cells cultured for 48 h alone (left two lanes) or together with the macrophages (MΦ), LSECs or HepG2 cells (above blot) in a Transwell system with (+) or without (–) stimulation with IFN-α (1,000 U/ml). Numbers below lanes indicate densitometry results throughout (presented (as %) relative to control, unstimulated, mock-treated or intact cells). RC, relaxed circular DNA; SS, single-stranded DNA. (**b**) Luciferase activity of HepG2 cells, HepG2.2.15 cells, macrophages and LSECs transfected with a ISRE luciferase reporter plasmid and a control luciferase plasmid and then left unstimulated (US) or stimulated for 12 h with IFN-α (key); results are presented relative to activity of the control luciferase plasmid. (**c**) Immunoblot analysis of total STAT1 (STAT1) and STAT1 phosphorylated at Tyr701 (p-STAT1) in HepG2.2.15 cells, macrophages and LSECs transduced with lentiviral vector expressing control shRNA with scrambled sequence (–) or STAT1-specific shRNA (+) and left untreated (Ctrl) or treated with IFN-α; β-actin serves as a loading control throughout. (**d**,**e**) Southern blot analysis of HBV replication (as in **a**) in HepG2.2.15 cells cultured with macrophages (**d**) or LSECs (**e**) transduced with shRNA-expressing lentiviral vector and left untreated or treated with IFN-α as in **c**. (**f**) PCR analysis of HBV DNA in the serum (top) and immunoblot analysis of total and phosphorylated STAT1 (as in **c**) in liver cells (bottom) of mice given hydrodynamic injection of various combinations of constructs (middle) for the expression of control (scrambled (Scr)) shRNA or STAT1-specific shRNA and a control vector (Ctrl) or vector for STAT1 expression driven by the CMV promoter or promoters specific for hepatocytes (HC), macrophages (MΦ) or endothelial cells (EC) and, 24 h later, treated for an additional 72 h with IFN-α or left not. AV, antiviral activity; KD, knockdown. (**g**) Immunoblot analysis of F4/80 in the liver of mice treated for 48 h with liposomal clodronate (CLL +) or not (CLL –) and then given no further treatment (left) or reconsitututed with BMDMs (+) or PBS (–) for an additional 72 h (right); two lanes per condition represent the same two mice throughout **g**. (**h**) PCR analysis of HBV DNA in serum from mice treated for 48 h with liposomal clodronate, then given adoptive transfer of BMDMs in which STAT1 was knocked down (STAT1 KD) or not (No KD), followed for 24 h later by hydrodynamic injection of the HBV replicon construct and no stimulation (–) or stimulation with mouse IFN-α (+) for an additional 48 h. $^*P < 0.05$ and $^{**}P < 0.01$ (Student's *t*-test). Data are representative of three (**a**,**c**–**e**) or two (**f** (bottom), **g**) independent experiments (with eight (**f**, bottom) or three (**g**) mice per group) or are from three independent experiments (**b**; mean and s.e.m.) or two independent experiments (**f** (top), **h**; mean and s.e.m. of eight (**f**) or four (**h**) mice per group).

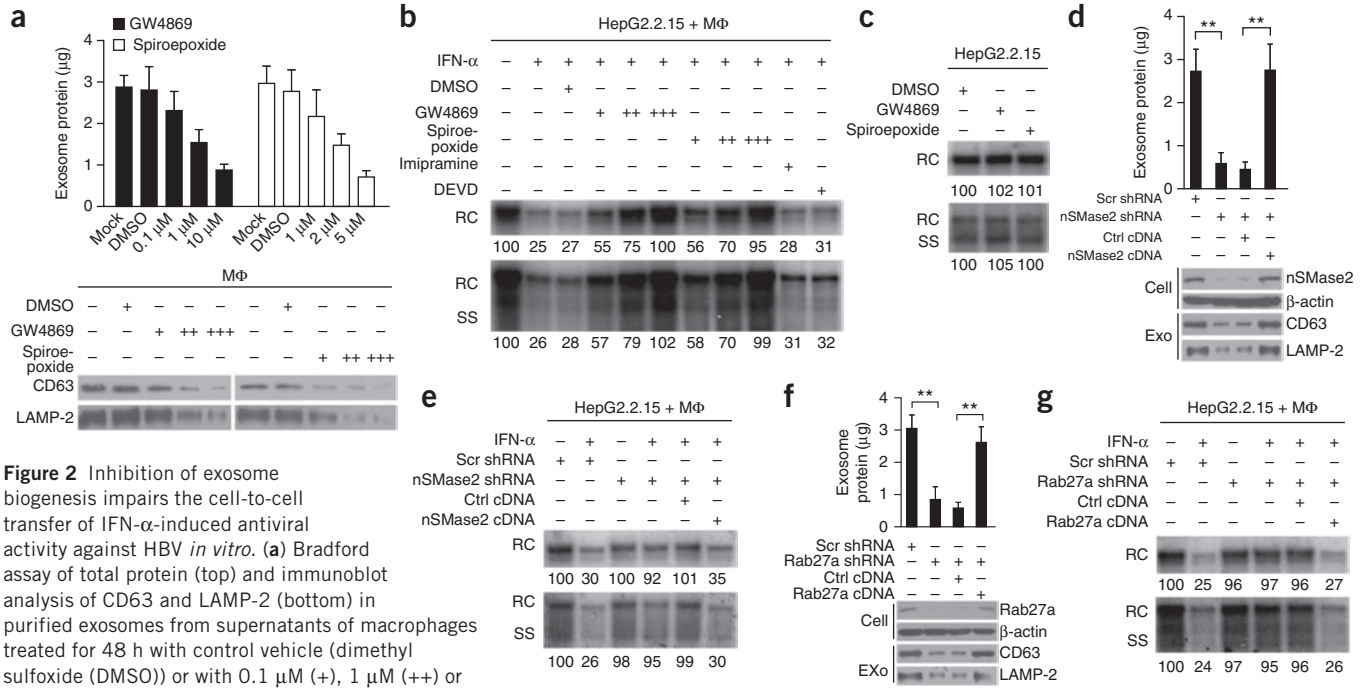

Figure 2 Inhibition of exosome biogenesis impairs the cell-to-cell transfer of IFN-α-induced antiviral activity against HBV *in vitro*. (**a**) Bradford assay of total protein (top) and immunoblot analysis of CD63 and LAMP-2 (bottom) in purified exosomes from supernatants of macrophages treated for 48 h with control vehicle (dimethyl sulfoxide (DMSO)) or with 0.1 μM (+), 1 μM (++) or 10 μM (+++) GW4869 or 1 μM (+), 2 μM (++) or 5 μM (+++) spiroepoxide. (**b**) Southern blot analysis of HBV replication (as in **Fig. 1a**) in HepG2.2.15 cells cultured with macrophages and treated with DMSO, GW4869 or spiroepoxide (as in **a**) or with imipramine (10 μM) or DEVD (60 μM), followed by treatment with IFN-α or not. (**c**) Southern blot analysis of HBV replication (as in **b**) in HepG2.2.15 cells treated for 48 h with DMSO, 10 μM GW4869 or 5 μM spiroepoxide. (**d**) Bradford assay of total protein in purified exosomes (top) and immunoblot analysis of nSMase2 in lysates (Cell) and of CD63 and LAMP-2 in purified exosomes (Exo; bottom) of macrophages transduced with lentiviral vectors for scrambled or nSMase2-specific shRNA, plus no cDNA, control vector cDNA (Ctrl cDNA) or siRNA-resistant nSMase2 cDNA (nSMase2 cDNA). (**e**) Southern blot analysis of HBV replication (as in **b**) in HepG2.2.15 cells cultured with macrophages transduced with lentiviral vectors as in **d**, followed by treatment with IFN-α or not. (**f**) Bradford assay (top) and immunoblot analysis (bottom) of exosomes from macrophages transduced with lentiviral vectors for scrambled or Rab27a-specific shRNA plus no cDNA, control cDNA or siRNA-resistant Rab27a cDNA (similar to **d**). (**g**) Southern blot analysis of HBV replication (as in **b**) in HepG2.2.15 cells cultured with macrophages transduced with lentiviral vectors as in **f**, followed by treatment with IFN-α or not. $*P < 0.05$ and $**P < 0.01$ (Student's *t*-test). Data are from three (**a**, top) or two (**d**,**f** (top)) independent experiments (mean and s.e.m.) or are representative of three (**a** (bottom), **b**) or two (**c**,**d**,**f** (bottom), **e**,**g**) independent experiments.

To elucidate the influence of LNPCs on the antiviral activity of IFN-α *in vivo*, we used a 'knockdown-and-rescue' strategy for STAT1 that entailed hydrodynamics-based transfection in a mouse model of acute infection with HBV[24]. We hydrodynamically injected a vector encoding short hairpin RNA (shRNA) targeting mouse STAT1 plus an HBV replicon construct into the tail vein of mice, together with a plasmid for the expression of STAT1 driven by the ubiquitous cytomegalovirus (CMV) promoter or a liver cell type–specific promoter, then treated the mice with IFN-α. We confirmed the specificity of the liver cell type–specific promoter in mice (**Supplementary Fig. 1e**). Knockdown of STAT1 expression greatly impaired the antiviral activity of IFN-α against HBV (**Fig. 1f**); that impaired activity was restored completely by the STAT1 expression plasmid driven by the CMV promoter but was restored only partially by a STAT1 expression plasmid driven by a hepatocyte-specific promoter (**Fig. 1f**). Notably, STAT1 expression vectors driven by a macrophage-specific promoter or an endothelial cell–specific promoter significantly restored the IFN-α-induced antiviral response, and this restoration was even greater when those vectors were used together (**Fig. 1f**). We confirmed the knockdown and restoration of STAT1 expression in total liver cells, hepatocytes, macrophages and LSECs by immunoblot analysis (**Fig. 1f**). Therefore, loss of IFN-α signaling in nonpermissive LNPCs such as macrophages or endothelial cells adversely affected control of the virus.

Next we used depletion and reconstitution of macrophages *in vivo* to further demonstrate the role of LNPCs in the IFN-α-induced suppression of HBV replication in hepatocytes. Consistent with a published report[25], we successfully achieved depletion of macrophages from mouse liver by treatment with clodronate-liposomes and reconstitution by adoptive transfer of bone marrow–derived macrophages (BMDMs), as verified by immunoblot analysis and confocal fluorescence imaging of the macrophage marker F4/80 in liver tissues (**Fig. 1g** and **Supplementary Fig. 1f**). HBV infection was less sensitive to IFN-α in mice that received adoptive transfer of BMDMs in which STAT1 was knocked down than in mice given control BMDMs without STAT1 knockdown (**Fig. 1h**). However, significant antiviral activity was still induced by IFN-α in mice repopulated with BMDMs in which STAT1 was knocked down (**Fig. 1h**); this might have been partially due to a contribution to such activity by cells other than macrophages, such as the endothelium (**Fig. 1f**). Together these data demonstrated an essential role for LNPCs in IFN-α-induced suppression of HBV replication in hepatocytes both *in vitro* and *in vivo*.

Exosomal transfer of IFN-α anti-HBV activity *in vitro*

To investigate the role of exosomes secreted from LNPCs in the transfer of the IFN-α-induced antiviral response to HBV in hepatocytes, we first blocked exosome production in macrophages in the *in vitro* Transwell coculture system by targeting neutral sphingomyelinase 2 (nSMase2), which has been shown to contribute to exosome secretion by triggering the budding of exosomes into MVBs[26]. Accordingly, two structurally unrelated inhibitors of nSMase2, GW4869 and spiroepoxide, which are well-known inhibitors of exosome release[9,26–28], inhibited

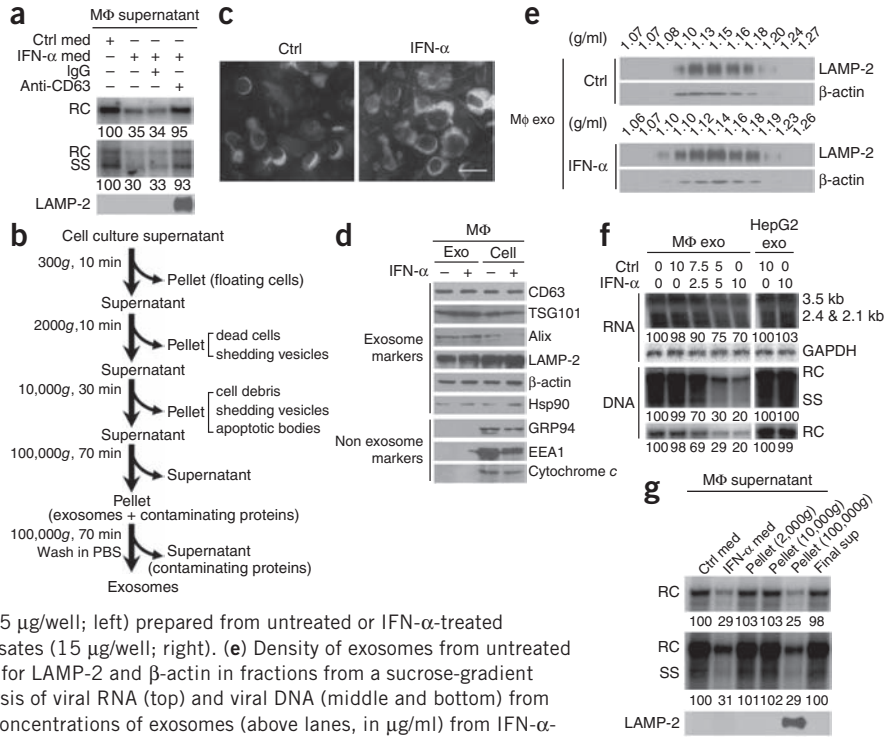

Figure 3 Exosomes are sufficient to mediate the transfer of an IFN-α-induced antiviral response *in vitro*. (**a**) Southern blot analysis of HBV replication (as in **Fig. 1a**) in HepG2.2.15 cells cultured with supernatants obtained from untreated macrophage-derived cells (Ctrl med) or with supernatants obtained from IFN-α-treated macrophage-derived cells, incubated with no antibody (IFN-α med), biotinylated antibody to CD63 (Anti-CD63) or control antibody (immunoglobulin G (IgG)) and subjected to 'immunodepletion' (removal of exosomes through the use of antibodies) with streptavidin beads before culture with the HepG2.2.15 cells (top two blots). Bottom, immunoblot analysis of LAMP-2 among proteins immunoprecipitated with anti-CD63. (**b**) Strategy for the isolation and purification of exosomes from culture supernatants based on differential ultracentrifugation. (**c**) Electron microscopy of purified exosomes from untreated macrophages (left) or IFN-α-treated macrophages (right). Scale bar, 100 nm. (**d**) Immunoblot analysis of exosomal and nonexosomal markers (along margins) in exosomes (5 μg/well; left) prepared from untreated or IFN-α-treated macrophages and in the corresponding whole-cell lysates (15 μg/well; right). (**e**) Density of exosomes from untreated or IFN-α-treated macrophages, assessed by probing for LAMP-2 and β-actin in fractions from a sucrose-gradient ultracentrifugation. (**f**) RNA and Southern blot analysis of viral RNA (top) and viral DNA (middle and bottom) from HepG2.2.15 cells treated for 48 h with increasing concentrations of exosomes (above lanes, in μg/ml) from IFN-α-stimulated macrophages (MΦ exo) or HepG2 cells (HepG2 exo), in combination with control exosomes (from unstimulated cells): 3.5 kb, HBV pregenomic RNA; 2.4 kb, HBV pre-S1 and S RNA; 2.1 kb, HBV pre-S2 and S RNA. GAPDH serves as an RNA loading control. (**g**) Southern blot analysis of HBV replication (as in **Fig. 1a**) in HepG2.2.15 cells treated with control medium, supernatant of IFN-α-treated macrophages, or pellets and final supernatant of sequential centrifugation of IFN-α-treated macrophages as in **b** (top and middle). Bottom. immunoblot analysis of LAMP-2 in those samples. Data are representative of two (**a**,**e**,**g**) or three (**c**,**d**,**f**) independent experiments.

the release of exosomes by the macrophages in a dose-dependent manner (**Fig. 2a**). The elimination of the IFN-α-induced inhibition of HBV replication by the chemical targeting of nSMase2 activity in the coculture system depended on the extent to which exosome release was inhibited (**Fig. 2b**). In contrast, treatment with imipramine or DEVD, which selectively block the secretion of shedding vesicles and apoptotic bodies[29,30] (two other widely studied extracellular vesicles[5,6]), respectively, did not affect the transmission of IFN-α-induced antiviral activity in the coculture system (**Fig. 2b**). GW4869 and spiroepoxide had no apparent direct effect on HBV propagation in HepG2.2.15 cells cultured alone (**Fig. 2c**).

As a complementary approach, we then transduced macrophages with shRNA targeting nSMase2. Consistent with published studies[9,26,27], knockdown of nSMase2 resulted in significantly less release of exosomes (**Fig. 2d**). The suppression of endogenous nSMase2 expression in the macrophages also restored HBV production in IFN-α-treated HepG2.2.15 cells to an amount similar to that of untreated cells (**Fig. 2e**). Moreover, ectopic expression of nSMase2 in cells in which nSMase2 was knocked down restored the IFN-α-induced antiviral state in cells in which HBV was replicating (**Fig. 2e**), which ruled out the possibility of off-target effects of the shRNA. The transfer of IFN-α-induced antiviral activity by the macrophages was also inhibited by shRNA-mediated silencing of the small GTPase Rab27a (**Fig. 2f**,**g**), which has been linked to the exosome-release pathway by its promoting the docking of MVBs to the plasma membrane[9,31].

To directly investigate the antiviral activity of exosomes derived from IFN-α-treated LNPCs, we first depleted supernatants of IFN-α-stimulated macrophages of exosomes through the use of antibody to CD63 (a membrane marker associated with exosomes)[32]. That depletion of exosomes considerably inhibited the antiviral activity of supernatants of IFN-α-stimulated macrophages (**Fig. 3a**). Immunoblot analysis of the proteins immunoprecipitated with antibody to CD63 identified the exosomal lysosome-associated membrane protein LAMP-2 (**Fig. 3a**), which verified successful 'immunocapture'. Next we isolated exosomes from IFN-α-stimulated or unstimulated macrophages by differential centrifugation[32] (**Fig. 3b**). We typically obtained 5–10 μg of exosome proteins from 1×10^6 cells. Stimulation with IFN-α did not significantly affect the yield of exosomes (data not shown). Electron microscopy of the purified pellets identified small membrane vesicles of up to 100 nm in diameter, with the cup-shaped structure typical of exosomes[5,32], whereas contaminating debris and noncircular membranes were absent from the pellets (**Fig. 3c**). Comparison of cell lysates with exosomal preparations showed the presence of the exosomal markers CD63, TSG101 and Alix, as well as several conserved exosomal proteins, including LAMP-2, β-actin and hsp90 (**Fig. 3d**). We confirmed the purity of the exosome samples by the absence of GRP94 (an endoplasmic reticulum marker), EEA1 (an endosomal marker) and cytochrome *c* (a mitochondrial marker) (**Fig. 3d**). Sucrose-gradient ultracentrifugation of the exosomal preparations indicated that LAMP-2 and β-actin were distributed mainly in the fractions with a buoyant density in sucrose of 1.10–1.19 g/ml (**Fig. 3e**), which corresponded to the density reported for exosomes[28,33]. Treatment of HepG2.2.15 cells with purified exosomes from IFN-α-treated macrophages resulted in slightly less viral RNA and a much lower abundance of intracellular nucleocapsid-associated DNA and extracellular enveloped viral DNA, in a dose-dependent manner (**Fig. 3f**), which suggested that intracellular viral RNA and DNA were both targeted by the exosomes derived from IFN-α-stimulated LNPCs. In contrast, the final supernatants of the

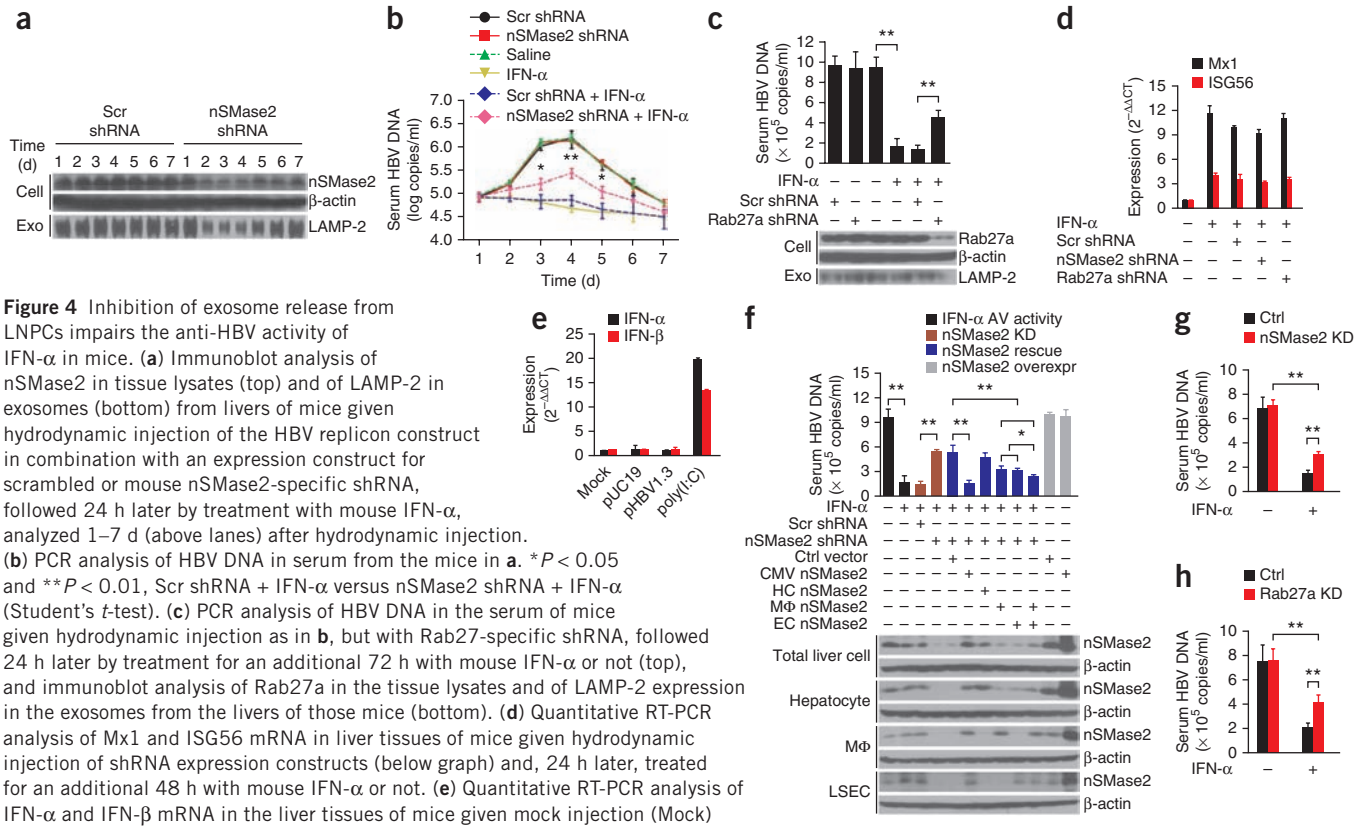

Figure 4 Inhibition of exosome release from LNPCs impairs the anti-HBV activity of IFN-α in mice. (**a**) Immunoblot analysis of nSMase2 in tissue lysates (top) and of LAMP-2 in exosomes (bottom) from livers of mice given hydrodynamic injection of the HBV replicon construct in combination with an expression construct for scrambled or mouse nSMase2-specific shRNA, followed 24 h later by treatment with mouse IFN-α, analyzed 1–7 d (above lanes) after hydrodynamic injection. (**b**) PCR analysis of HBV DNA in serum from the mice in **a**. $*P < 0.05$ and $**P < 0.01$, Scr shRNA + IFN-α versus nSMase2 shRNA + IFN-α (Student's *t*-test). (**c**) PCR analysis of HBV DNA in the serum of mice given hydrodynamic injection as in **b**, but with Rab27-specific shRNA, followed 24 h later by treatment for an additional 72 h with mouse IFN-α or not (top), and immunoblot analysis of Rab27a in the tissue lysates and of LAMP-2 expression in the exosomes from the livers of those mice (bottom). (**d**) Quantitative RT-PCR analysis of Mx1 and ISG56 mRNA in liver tissues of mice given hydrodynamic injection of shRNA expression constructs (below graph) and, 24 h later, treated for an additional 48 h with mouse IFN-α or not. (**e**) Quantitative RT-PCR analysis of IFN-α and IFN-β mRNA in the liver tissues of mice given mock injection (Mock) or hydrodynamic injection for 24 h of control plasmid (pUC19), the HBV replicon construct (pHBV1.3) or an interferon inducer (poly(I:C)). (**f**) PCR analysis of HBV DNA in the serum (top) and immunoblot analysis of nSMase2 in liver cells (bottom) of mice given hydrodynamic injection of constructs for the expression of control or nSMase2-specific shRNA and control vector or vector for nSMase2 expression driven by various promoters (as in **Fig. 1f**) and, 24 h later, treated for an additional 72 h with mouse IFN-α or not. (**g**,**h**) PCR analysis of HBV DNA in the serum of mice depleted of macrophages by liposomal clodronate and, 24 h later, given adoptive transfer of control BMDMs (Ctrl) or BMDMs in which STAT1 (**g**) or Rab27a (**h**) was knocked down, followed by hydrodynamic injection of the HBV replicon construct (15 μg) and stimulation for an additional 48 h with mouse IFN-α or not. $*P < 0.05$ and $**P < 0.01$ (Student's *t*-test). Data are representative of two independent experiments with four to eight mice per group (**a**,**c**,**f** (bottom)) or are from two independent experiments with four to eight mice per group (**b**–**h**; mean and s.e.m.).

sequential centrifugation of IFN-α-stimulated macrophages and the resultant pellets without exosomes did not have any antiviral activity (**Fig. 3g**). Similar to their parent cells, exosomes derived from IFN-α-stimulated HepG2 cells showed no antiviral activity against HBV (**Fig. 3f**). The inhibition of HBV replication by exosomes derived from IFN-α-stimulated macrophages was not due to enhanced apoptosis or diminished viability of HepG2.2.15 cells (data not shown).

We obtained similar results with another type of LNPC, LSECs (**Supplementary Fig. 2a–f** and **Supplementary Fig. 3a–f**), which indicated that the exosome-mediated transfer of IFN-α-induced antiviral activity was specific to the cell type but was not limited to macrophages. We found that the exosomes from IFN-α-treated macrophages and LSECs greatly restricted the replication of another liver-tropic virus, hepatitis C virus (HCV) (**Supplementary Fig. 4a–f**), which suggested that the exosome-mediated antiviral mechanism of IFN-α may also apply to HCV. Together these data indicated that exosomes from LNPCs were necessary and sufficient to mediate the transfer of the IFN-α-induced antiviral response to hepatocyte-derived cells *in vitro*.

Exosomal transfer of IFN-α antiviral activity *in vivo*

To confirm the exosome-mediated transmission of antiviral activity from LNPCs to hepatocytes *in vivo*, we first hydrodynamically injected an expression vector encoding mouse nSMase2–specific shRNA into the tail vein, along with the HBV replicon construct, then treated the mice with IFN-α. The expression of nSMase2 and release of exosomes in the liver were inhibited substantially by nSMase2-specific shRNA from day 2 to day 4 after injection and then gradually recovered starting on day 5 (**Fig. 4a**). The nSMase2-specific shRNA inhibited (by approximately 20–50%) IFN-α-induced antiviral activity against HBV from day 3 to day 5 relative to activity detected after treatment with control shRNA, and this inhibitory effect disappeared with the recovery of nSMase2 expression and exosome release (**Fig. 4b**). Knockdown of the expression of Rab27a resulted in a similar inhibitory effect on IFN-α-induced antiviral activity in mice (**Fig. 4c**). The impaired control of virus by IFN-α in mice given injection of nSMase2-specific or Rab27a-specific shRNA was not a result of less ISG induction, as demonstrated by the unaltered expression of interferon-inducible Mx1 mRNA and ISG56 mRNA in the liver tissues (**Fig. 4d**). Notably, mice given injection of nSMase2-specific or Rab27a-specific without exogenous IFN-α treatment did not have enhanced viral replication (**Fig. 4b**,**c**), possibly because HBV could not induce interferon production in the mice (**Fig. 4e**).

We next used vectors for nSMase2 expression driven by ubiquitous or cell type–specific promoters to restore nSMase2 expression in mice given injection of nSMase2-specific shRNA. The impaired antiviral activity of IFN-α resulting from nSMase2-specific shRNA was completely reversed by the CMV promoter–driven nSMase2 expression vector (**Fig. 4f**). The restoration of nSMase2 expression in macrophages or LSECs significantly restored the IFN-α-induced antiviral

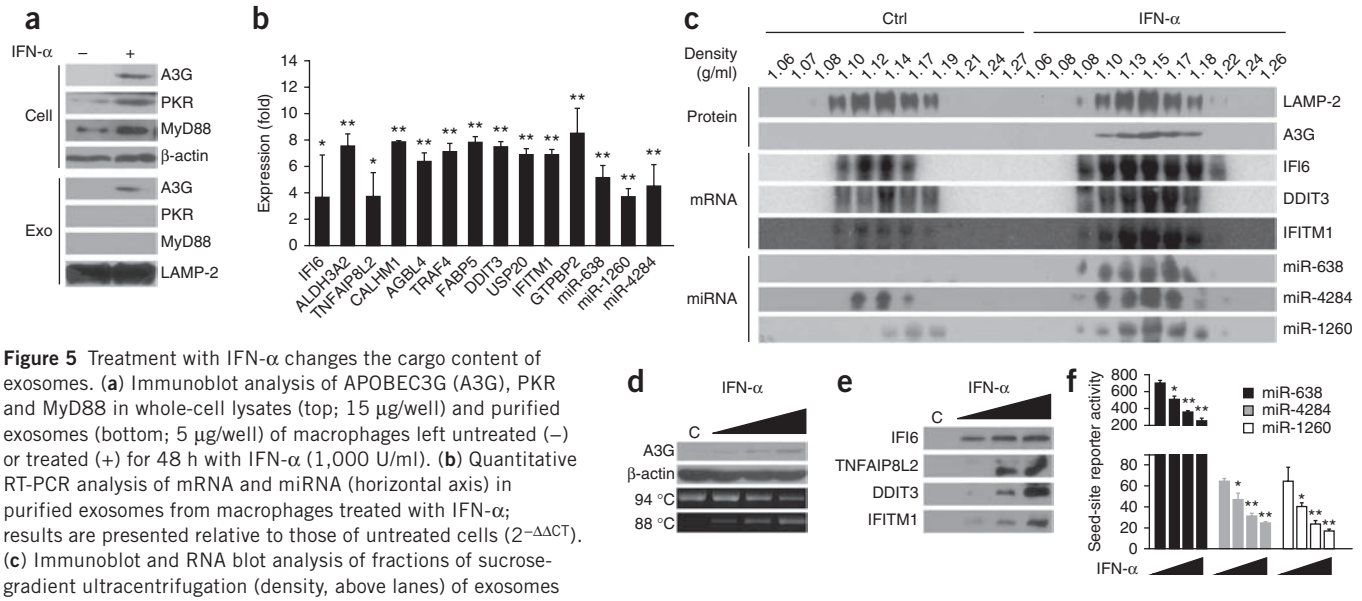

Figure 5 Treatment with IFN-α changes the cargo content of exosomes. (**a**) Immunoblot analysis of APOBEC3G (A3G), PKR and MyD88 in whole-cell lysates (top; 15 μg/well) and purified exosomes (bottom; 5 μg/well) of macrophages left untreated (–) or treated (+) for 48 h with IFN-α (1,000 U/ml). (**b**) Quantitative RT-PCR analysis of mRNA and miRNA (horizontal axis) in purified exosomes from macrophages treated with IFN-α; results are presented relative to those of untreated cells ($2^{-\Delta\Delta CT}$). (**c**) Immunoblot and RNA blot analysis of fractions of sucrose-gradient ultracentrifugation (density, above lanes) of exosomes derived from untreated (Ctrl) or IFN-α-treated (IFN-α) macrophages. (**d**) Immunoblot analysis of APOBEC3G (top) and PCR analysis of HBV DNA at a denaturation temperature of 94 °C or 88 °C (bottom) in HepG2.2.15 cells incubated for 24 h with exosomes from unstimulated macrophages (C) or increasing amounts (wedge) of exosomes from IFN-α-stimulated macrophages (IFN-α). (**e**) Immunoblot analysis of the translation products of exosomal mRNA in HepG2.2.15 cells transfected for 24 h with increasing amounts of exosomal RNA from macrophages as in **d**. (**f**) Luciferase activity of miRNA seed-site reporters in HepG2.2.15 cells transfected for 12 h with each reporter plasmid and a control luciferase plasmid and then incubated for an additional 48 h with increasing concentrations of exosomes from IFN-α-stimulated macrophages. $^*P < 0.05$ and $^{**}P < 0.01$ (Student's *t*-test). Data are representative of two independent experiments (**a**,**c**–**e**) or are from two independent experiments (**b**,**f**; mean and s.e.m).

response, but restoration of nSMase2 expression in hepatocytes did not, and that restoration of the antiviral response was even greater when both the macrophages and LSECs were 'rescued' at the same time (**Fig. 4f**). The reversal of the impaired antiviral activity of IFN-α was not due to overcompensation of nSMase2 expression, as injection of the CMV promoter–driven nSMase2 expression vector alone and without IFN-α did not inhibit HBV replication (**Fig. 4f**). We confirmed the knockdown and restoration of nSMase2 expression in the total liver cells, hepatocytes, macrophages and LSECs by immunoblot analysis (**Fig. 4f**). Finally, we demonstrated that IFN-α induced a weaker antiviral response to HBV in mice repopulated with BMDMs in which nSMase2 or Rab27a was knocked down than in mice given control BMDMs (with no knockdown), after depletion of macrophages in the recipient mouse livers (**Fig. 4g**,**h**). However, because mice were depleted only of macrophages, we still observed antiviral activity of IFN-α in mice that received BMDMs in which nSMase2 or Rab27a was knocked down (**Fig. 4g**,**h**). The impaired antiviral response was due mostly to the inhibition of exosome secretion, as exosomes derived from IFN-α-stimulated control BMDMs (with no knockdown) restored the antiviral activity *in vitro* of the supernatants of BMDMs in which nSMase2 or Rab27a was knocked down (data not shown). Collectively, these results indicated that exosomes from LNPCs enhanced IFN-α-induced antiviral activity *in vivo*.

IFN-α-induced exosomal sorting of anti-HBV molecules

Exosomes can transfer functionally active protein, mRNA and miRNA between cells and thereby modify or reprogram the target cells[5,6]. We used immunoblot analysis to identify exosomal proteins with different expression in exosomes from IFN-α-treated LNPCs versus those from untreated LNPCs. We assessed the expression of APOBEC3G (a cytidine deaminase specific for single-stranded DNA), PKR (a protein kinase activated by double-stranded RNA) and MyD88 (a key adaptor in the signaling cascade of the innate immune response), which can be induced by IFN-α and has been reported to restrict HBV replication[17,34,35]. Although IFN-α induced the expression of APOBEC3G, PKR and MyD88 in macrophages and LSECs, treatment with IFN-α resulted in the 'sorting' of APOBEC3G, but not of MyD88 or PKR, into exosomes (**Fig. 5a** and **Supplementary Fig. 5a**).

Next we identified mRNA and miRNA with different expression in exosomes from IFN-α-stimulated LSECs versus those from unstimulated LSECs, by microarray. Among the differences in expression of mRNA and miRNA identified as significant by analysis of variance (ANOVA), we observed differences greater than 1.5-fold for 1,548 mRNAs and 22 miRNAs (**Supplementary Table 1**). Of those, 618 mRNAs and 3 miRNAs were more abundant in exosomes from IFN-α-treated LSECs than in those from untreated LSECs. To confirm the microarray data, we randomly selected 11 mRNAs from the 618 mRNAs and, together with the 3 miRNAs noted above (**Supplementary Table 2**), assessed these by quantitative PCR. We confirmed the greater abundance of those mRNAs and miRNAs in exosomes from IFN-α-stimulated LSECs (**Supplementary Fig. 5b**). We also observed a greater abundance of the 11 mRNAs and 3 miRNAs in exosomes from IFN-α-treated macrophages than in those from untreated macrophages (**Fig. 5b**), which indicated a common mechanism for the selective sorting of exosomes with specific mRNAs and miRNAs during stimulation with IFN-α. Furthermore, we confirmed the IFN-α-induced higher expression of a few of the molecules noted above in the exosomes of macrophages and LSECs by sucrose-gradient ultracentrifugation of exosomal preparations (**Fig. 5c** and **Supplementary Fig. 5c**). However, the changes in the exosomal mRNAs and miRNAs did not entirely reflect cellular changes, as IFN-α did not globally induce the expression of those mRNAs and miRNAs in the donor cells (**Supplementary Fig. 5d**,**e**), which suggested 'preferential sorting' of specific exosomal cargo.

We then examined the functionality of the molecules introduced by the exosomes. To verify the deaminase activity of APOBEC3G, we

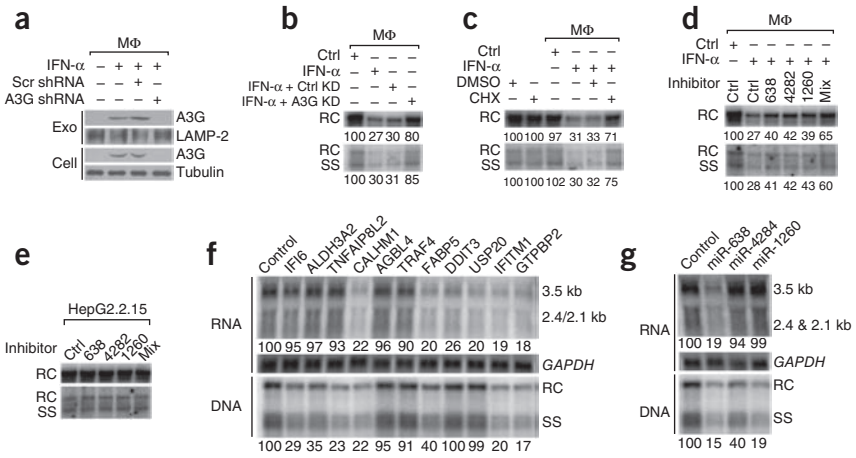

Figure 6 Exosomal molecules with different expression restrict HBV replication. (**a**) Immunoblot analysis of APOBEC3G in exosomes (top) and whole-cell lysates (bottom) of macrophages transduced with lentiviral vector for expression of scrambled or APOBEC3G-specific shRNA and left untreated or treated with IFN-α. (**b**) Southern blot analysis of HBV replication (as in **Fig. 1a**) in HepG2.2.15 cells incubated for 48 h with exosomes (5 μg/ml) derived from unstimulated or IFN-α-stimulated macrophages without shRNA (Ctrl and IFN-α, respectively) or from IFN-α-stimulated macrophages treated with control shRNA (IFN-α + Ctrl KD) or APOBEC3G-specific shRNA (IFN-α + A3G KD). (**c**,**d**) Southern blot analysis of HBV replication (as in **b**) in HepG2.2.15 cells treated for 2 h with DMSO or cycloheximide (CHX (10 μg/ml) (**c**) or transfected for 12 h with control (Ctrl) or specific miRNA inhibitors (above lanes) alone or in combination (Mix; 50 nM each) (**d**), followed by incubation for an additional 24 h (**c**) or 48 h (**d**) with exosomes (5 μg/ml) from unstimulated or IFN-α-stimulated macrophages, or no exosomes (**c**, left two lanes). (**e**) Southern blot analysis of HBV replication (as in **b**) in HepG2.2.15 cells transfected for 48 h with miRNA inhibitors alone or in combination (as in **d**). (**f**,**g**) RNA and Southern blot analysis of viral RNA (top) and nucleocapsid-associated DNA (bottom) in HepG2 cells transfected for 48 h with individual expression vectors for mRNA (4 μg each) (**f**) or individual miRNA mimics (50 nM each) (**g**) in combination with the HBV replicon construct (2 μg). Data are representative of two (**a**,**e**) or three (**b**–**d**,**f**,**g**) independent experiments.

incubated HepG2.2.15 cells with exosomes from IFN-α-stimulated macrophages and LSECs. Amplification of viral DNA at a low denaturation temperature of 88 °C resulted in positive signals, the intensity of which was associated with APOBEC3G expression (**Fig. 5d** and **Supplementary Fig. 5f**); this indicated that cytosine deamination occurred. Furthermore, we transfected the HepG2.2.15 cells with exosome-derived total RNA and with or without miRNA 'seed-site' reporters. We observed a dose-dependent increase in the abundance of the translated products of selected exosomal mRNAs (**Fig. 5e** and **Supplementary Fig. 5g**) and a dose-dependent suppression of luciferase activity for the miRNA reporters (**Fig. 5f** and **Supplementary Fig. 5h**), which suggested that the exosome-shuttled RNA molecules were functional.

To investigate the contributions of the functional APOBEC3G, mRNA and miRNA populations to the exosome-mediated antiviral activity of IFN-α, we knocked down APOBEC3G expression in macrophages, inhibited translation of exosomal mRNA with cycloheximide and blocked miRNA function through the use of miRNA inhibitors alone or in combination. APOBEC3G-specific shRNA resulted in much less IFN-α-induced 'sorting' of APOBEC3G in the exosomes (**Fig. 6a**). Moreover, knockdown of APOBEC3G and inhibition of mRNA translation greatly impaired the antiviral activity of exosomes from IFN-α-treated macrophages (**Fig. 6b**,**c**). Individual miRNA inhibitors slightly restored the production of virus, whereas miRNA inhibitors used in combination efficiently restored the production of virus (**Fig. 6d**). Such restoration of the production of virus was not due to direct enhancement of viral replication by the miRNA inhibitors (**Fig. 6e**). In addition, the antiviral activity of exosomes derived from IFN-α-treated LSECs was impaired by the APOBEC3G-specific shRNA, cycloheximide and the three miRNA inhibitors (**Supplementary Fig. 6a**–**d**).

To demonstrate the direct inhibitory effects on HBV replication of the exosomal molecules with different expression, we transfected HepG2 cells with expression vectors for the 11 selected mRNAs and mimics of the 3 selected miRNAs (**Supplementary Table 2**), together with the HBV replicon construct. We then measured intracellular viral RNA and DNA by RNA and Southern blot analysis, respectively. CALHM1, FABP5, DDIT3, USP20, IFITM1, GTPBP2 and the miRNA hsa-miR-638 greatly suppressed the abundance of viral RNA (**Fig. 6f**,**g**). Replication of HBV DNA was inhibited concurrently by FABP5, IFITM1, GTPBP2 and hsa-miR-638 but not by DDIT3 or USP20 (**Fig. 6f**,**g**), which indicated that DDIT3 and USP20 enhanced viral DNA replication in addition to affecting the transcription of viral RNA. Moreover, IFI6, ALDH3A2, TNFAIP8L2 and the miRNAs hsa-miR-4284 and hsa-miR-1260 moderately or substantially inhibited replication of HBV DNA (**Fig. 6f**,**g**). We confirmed by immunoblot analysis that the proteins encoded were expressed in the transfected cells (**Supplementary Fig. 6e**). Collectively, these findings demonstrated that some of the exosomal molecules with different expression were responsible for the exosome-mediated antiviral activity of IFN-α.

IFN-α-induced exosomal transfer of anti-HBV molecules

To determine whether exosomes shed by LNPCs were able to shuttle antiviral molecules to hepatocytes after stimulation with IFN-α, we labeled purified exosomes from unstimulated and IFN-α-stimulated macrophages with the green fluorescent lipid dye PKH67 or the green RNA-selective nucleic acid stain SYTO RNASelect. We then cultured those exosomes for 2 h with HepG2.2.15 cells and then analyzed by confocal microscopy the internalization of exosomes by HepG2.2.15 cells. The exosomes (including membrane and RNA cargo) were efficiently internalized by the HepG2.2.15 cells (**Fig. 7a**), whereas annexin V, which is reported to block phosphatidylserine at the exosome surface and thereby inhibit exosome internalization[11,36], diminished exosome internalization and the antiviral activity of exosomes from IFN-α-stimulated macrophages (**Fig. 7b**,**c**).

Next we cultured HepG2.2.15 cells together with macrophages with or without treatment with IFN-α. Treatment with IFN-α resulted in substantial upregulation of APOBEC3G expression in the cocultured macrophages and HepG2.2.15 cells but not in HepG2.2.15 cells cultured alone (**Fig. 7d**), which indicated transfer of APOBEC3G from the macrophages to the HepG2.2.15 cells. That transfer was impaired by the exosome-release inhibitor GW4869 and internalization inhibitor annexin V (**Fig. 7d**). Consistent with those findings, we observed similar exosome-mediated transfer of IFI6 mRNA, TNFAIP8L2 mRNA, DDIT3 mRNA, IFITM1 mRNA and hsa-miR-638 from macrophages

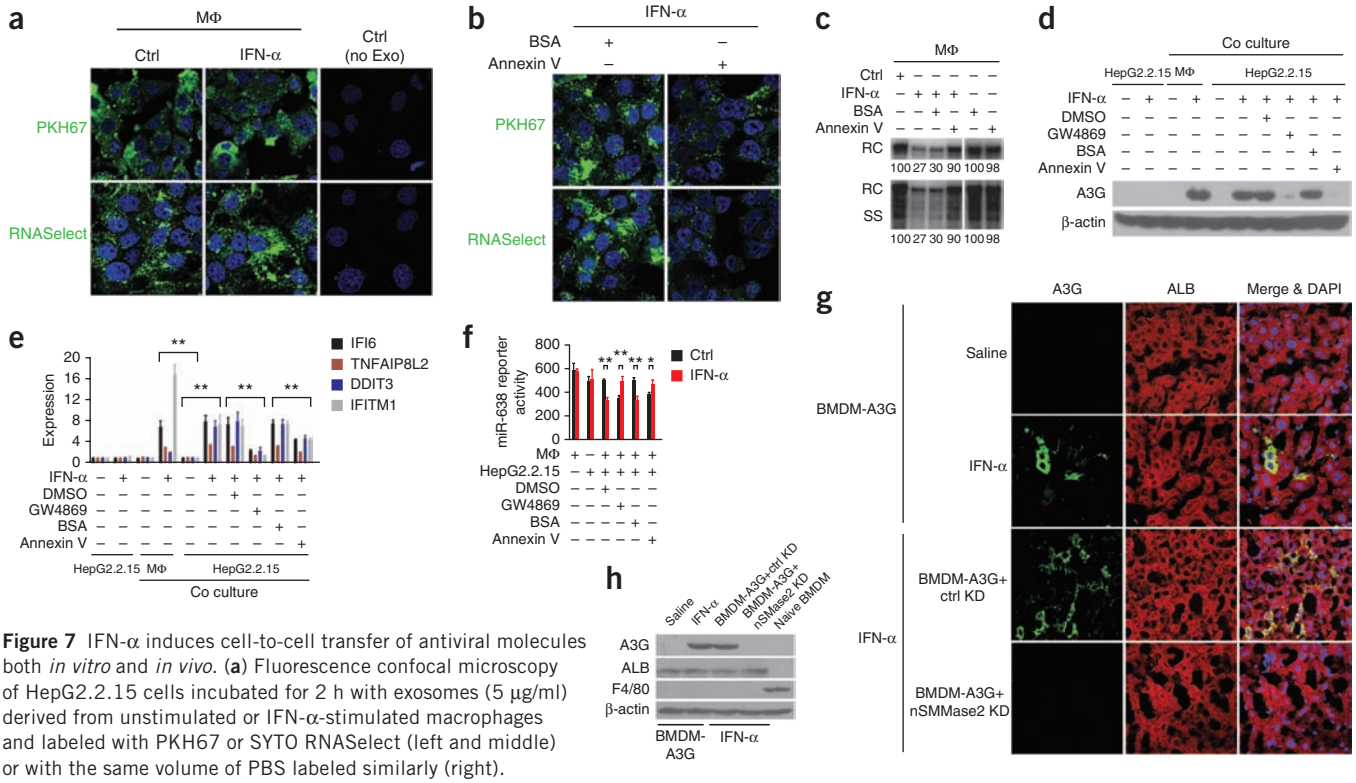

Figure 7 IFN-α induces cell-to-cell transfer of antiviral molecules both *in vitro* and *in vivo*. (**a**) Fluorescence confocal microscopy of HepG2.2.15 cells incubated for 2 h with exosomes (5 μg/ml) derived from unstimulated or IFN-α-stimulated macrophages and labeled with PKH67 or SYTO RNASelect (left and middle) or with the same volume of PBS labeled similarly (right). (**b**) Fluorescence confocal microscopy of HepG2.2.15 cells treated for 2 h with exosomes derived from IFN-α-stimulated macrophages and labeled as in **a**, then preincubated for 2 h with annexin V (2 μg/ml) or BSA before culture with HepG2.2.15 cells. (**c**) Southern blot analysis of HBV replication (as in **Fig. 1a**) in HepG2.2.15 cells treated for 48 h with exosomes (5 μg/ml) obtained from unstimulated or IFN-α-stimulated or macrophages and preincubated as in **b** before addition to HepG2.2.15 cells. (**d**) Immunoblot analysis of APOBEC3G in HepG2.2.15 cells cultured alone (left two lanes) or cultured with macrophages incubated for 48 h with or without IFN-α (1,000 U/ml) in the presence of DMSO, GW4869 (10 μM), BSA or annexin V (2 μg/ml). (**e**) Quantitative RT-PCR analysis of mRNA (key) in HepG2.2.15 cells and macrophages treated as in **d**. (**f**) Luciferase activity of the miRNA-638 seed-site reporter in HepG2.2.15 cells and macrophages transfected for 12 h with the reporter and then treated as in **d**. (**g**) Fluorescence confocal microscopy of the localization of eGFP-APOBEC3G (detected with anti-GFP) and of albumin (ALB) in hepatocytes from mice given adoptive transfer of BMDMs transduced with lentiviral vector expressing eGFP-APOBEC3G (BMDM-A3G) alone, with or without IFN-α (top two rows), or together with lentiviral vector expressing control shRNA (ctrl KD) or nSMase2-specific shRNA (nSMase2 KD) and then, 24 h later, stimulated for an additional 24 h with mouse IFN-α (bottom two rows). DAPI, DNA-intercalating dye. (**h**) Immunoblot analysis of eGFP-APOBEC3G in cells treated as in **g**, or of naive BMDMs (positive control for anti-F4/80), probed with anti-GFP (A3G), anti-albumin (ALB) and anti-F4/80. Original magnification (**a**,**b**,**g**), ×400. $^{*}P < 0.05$ and $^{**}P < 0.01$ (Student's *t*-test). Data are representative of two independent experiments (**a**–**d**) or two independent experiments with three mice per group (**g**,**h**) or are from two independent experiments (**e**,**f**; mean and s.e.m.).

to HepG2.2.15 cells (**Fig. 7e**,**f**). In addition, we extended our study to LSECs and obtained similar results (**Supplementary Fig. 7a**–**f**).

To explore the exosome-mediated transmission of antiviral molecules *in vivo*, we transduced BMDMs with lentivirus expressing APOBEC3G tagged with enhanced green fluorescent protein under the control of the promoter of the gene encoding APOBEC3G (eGFP-APOBEC3G), either alone or in combination with lentivirus expressing nSMase2-specific shRNA. We confirmed that the transduced BMDMs released exosomes containing eGFP-APOBEC3G after stimulation with IFN-α *in vitro* (**Supplementary Fig. 7g**). IFN-α-induced APOBEC3G was transmitted from adoptively transferred BMDMs to hepatocytes in the mouse liver, as demonstrated by colocalization of eGFP-APOBEC3G and the hepatocyte marker albumin (**Fig. 7g**). The presence of nSMase2-specific shRNA prevented that transfer (**Fig. 7g**). Furthermore, we confirmed the transfer by the expression of eGFP-APOBEC3G in isolated hepatocytes (**Fig. 7h**). We verified the identity of the isolated hepatocytes by the presence of albumin and demonstrated the purity of the preparation by the absence of the macrophage marker F4/80 (**Fig. 7h**). Together these data showed that IFN-α induced the cell-to-cell transfer of antiviral molecules via exosomes both *in vitro* and *in vivo*.

IFN-α-induced control of other viruses via exosomes

To investigate whether exosomes had a role in the interferon-induced antiviral response to other viruses *in vivo*, we first studied mice infected with MHV-A59, a hepatotropic and neurotropic mouse hepatitis virus that can cause acute hepatitis and encephalitis[37]. We hydrodynamically injected an expression vector for mouse nSMase2–specific shRNA into mice, followed by injection of MHV-A59 alone or in combination with antibodies that neutralize IFN-α and IFN-β (collectively called 'IFN-α/β' here). The nSMase2-specific shRNA promoted the survival of MHV-A59 in mouse liver, as demonstrated by the higher concentration of alanine aminotransferase in the serum (**Fig. 8a**) and higher viral titers in the liver tissues (**Fig. 8b**). IFN-α/β-neutralizing antibodies rendered the exosome-mediated protective action redundant (**Fig. 8a**,**b**), which indicated that exosomes functioned in a manner dependent on IFN-α/β. We confirmed the effectiveness of the IFN-α/β-neutralizing antibodies by measuring Mx1 mRNA and ISG56 mRNA in the liver tissues (**Fig. 8c**). The impaired control of virus was not caused by lower expression of mRNA encoding effectors of the innate immune system, as demonstrated by the unaltered expression of mRNA encoding IFN-α, IFN-β, Mx1 or ISG56 (**Fig. 8c**).

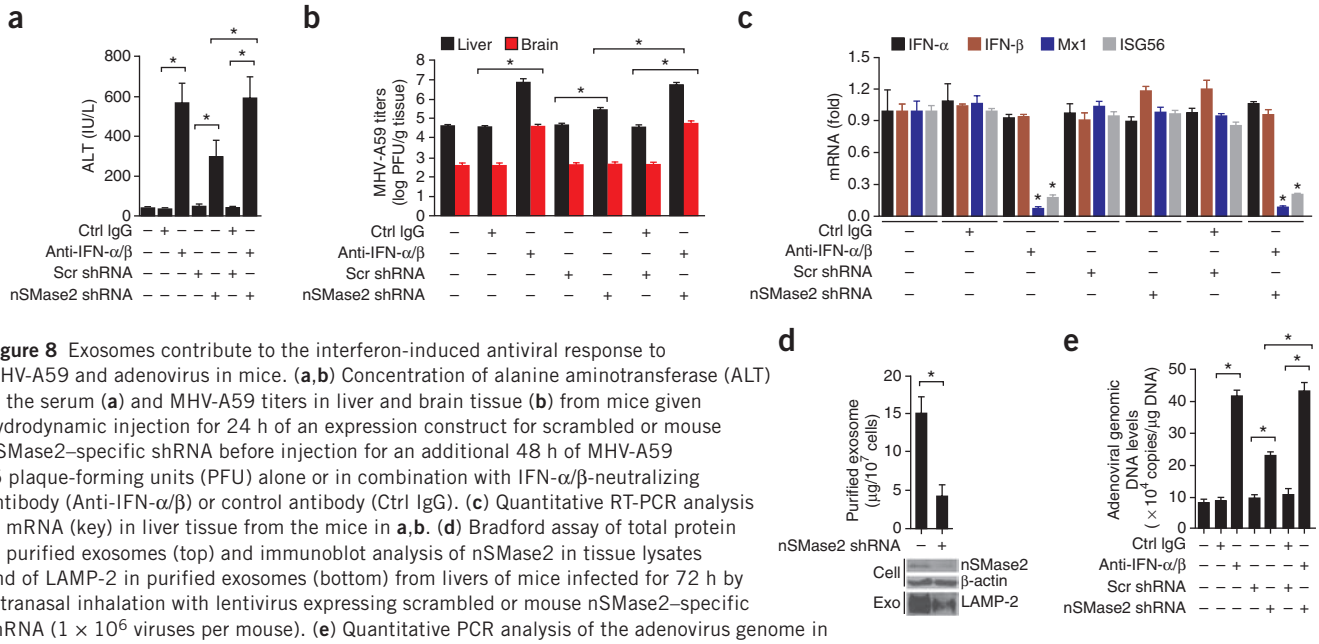

Figure 8 Exosomes contribute to the interferon-induced antiviral response to MHV-A59 and adenovirus in mice. (**a**,**b**) Concentration of alanine aminotransferase (ALT) in the serum (**a**) and MHV-A59 titers in liver and brain tissue (**b**) from mice given hydrodynamic injection for 24 h of an expression construct for scrambled or mouse nSMase2–specific shRNA before injection for an additional 48 h of MHV-A59 (5 plaque-forming units (PFU) alone or in combination with IFN-α/β-neutralizing antibody (Anti-IFN-α/β) or control antibody (Ctrl IgG). (**c**) Quantitative RT-PCR analysis of mRNA (key) in liver tissue from the mice in **a**,**b**. (**d**) Bradford assay of total protein in purified exosomes (top) and immunoblot analysis of nSMase2 in tissue lysates and of LAMP-2 in purified exosomes (bottom) from livers of mice infected for 72 h by intranasal inhalation with lentivirus expressing scrambled or mouse nSMase2–specific shRNA (1×10^6 viruses per mouse). (**e**) Quantitative PCR analysis of the adenovirus genome in lung tissue from mice infected for 24 h with lentivirus as in **d**, followed by intravenous injection of antibodies as in **a**,**b** and intranasal infection for an additional 72 h with MHV-A59 (1×10^9 plaque-forming units). $^*P < 0.01$ (Student's *t*-test). Data are from two independent experiments with six to eight mice per group (**a**–**e**; mean and s.e.m.) or are representative of two independent experiments with eight mice per group (**d**).

To determine whether the exosome-mediated antiviral response of endogenous IFN-α occurred in tissues other than liver, we used a model of infection of mouse lung with adenovirus[38]. We intranasally infected mice with lentivirus expressing nSMase2-specific shRNA to inhibit the release of exosomes in lung tissue, then administered recombinant adenovirus intranasally. The release of exosomes in lung tissue was markedly inhibited after knockdown of nSMase2 (**Fig. 8d**). That inhibition of exosome release significantly impaired the IFN-α-induced antiviral response to the adenovirus (**Fig. 8e**). Again, knockdown of nSMase2 did not alter the expression of effectors of the innate immune response (data not shown). The inhibition of exosome release by knockdown of Rab27a also impaired the endogenous IFN-α-induced antiviral response in models of infection with MHV-A59 or adenovirus (**Supplementary Fig. 8a–d**). Collectively, these results demonstrated that exosomes mediated the antiviral activity of endogenous IFN-α *in vivo*. Together our findings suggested that exosomes mediated the transmission of an IFN-α-induced antiviral response from nonpermissive LNPCs to HBV-permissive hepatocytes via exosomes and thus restored the antiviral state in hepatocytes (**Supplementary Fig. 9**).

DISCUSSION

In this study, we have presented evidence that IFN-α induced the transfer of antiviral molecules from LNPCs to hepatocytes through the release and internalization of exosomes. This intercellular transfer of exosomes bypassed the viral inhibition of interferon-induced expression of genes encoding antiviral molecules and resulted in restoration of the antiviral state in virus-infected cells. Our identification of this exosome-mediated antiviral effect of IFN-α signaling may provide a basis for therapeutic strategies to control viral infection.

The innate immune response to viruses involves the type I interferon–induced upregulation of the expression of cellular antiviral molecules[1]. To evade that interferon-mediated antiviral effect, viruses have evolved mechanisms to block the production and activity of interferon in virus-infected cells[3]. This raises the question of why the interferon-induced antiviral response is still able to control most if not all viral infections in the absence of adaptive immunity. Studies with an *in vitro* coculture system have demonstrated that HCV RNA can be transferred from infected hepatocytes by exosomes to plasmacytoid dendritic cells (pDCs) to trigger interferon production[28,39], which indicates that interferon is produced in the liver by pDCs rather than by HCV-infected hepatocytes. One of the most notable observations of those studies is that interferon induction by pDCs is dependent on direct cell-to-cell contact with infected hepatocytes[28,39]; this suggests that interferon production by pDCs requires an abundance of viral RNA, which is transferred to the pDCs by exosomes.

We demonstrated here that IFN-α induced cell-to-cell transfer of resistance to HBV replication. The cultivation of macrophages or LSECs together with cells in which HBV was able to replicate resulted in the inhibition of HBV replication after stimulation with IFN-α, in a manner dependent on exosomes but independent of direct cell contact. This suggested that uninfected cells adjacent to infected cells were able to efficiently confer the antiviral activity of IFN-α on the infected cells via exosomes. Thus, although many viruses have developed strategies to evade interferon in infected cells, neighboring cells could help to restore the antiviral state in infected cells through exosome-mediated transfer mechanisms.

Because specific inhibition of STAT1 expression and exosome release in LNPCs significantly weakened the IFN-α-induced antiviral response to HBV *in vivo*, we conclude that IFN-α both targeted virus-infected cells to directly limit viral replication and acted on virus-resistant or uninfected cells to indirectly inhibit viral infection via the exosome-mediated transfer of antiviral activity. However, silencing STAT1 expression in the HepG2.2.15 cells did not blunt the macrophage- and LSEC-mediated anti-HBV activity of IFN-α in the HepG2.2.15 cells, which might have been due to the substantial replication of HBV in the HepG2.2.15 cells and the low sensitivity to IFN-α of the HepG2.2.15 cells[20]. Thus, the relative importance of these two antiviral mechanisms of IFN-α might depend on the complicated virus-host interaction. We demonstrated that both macrophages

and LSECs contributed to the exosome-induced antiviral activity of IFN-α against HBV; however, whether other LNPCs are also involved in the response remains unclear. Our observations seemed to suggest that exosomes from uninfected hepatocytes did not mediate the anti-HBV effect of IFN-α. Other experiments indicated that HepG2 cells released fewer exosomes than did macrophages or LSECs (data not shown) and that even an equal amount of exosomes from IFN-α-treated HepG2 cells showed no anti-HBV activity, in contrast to exosomes from IFN-α-treated macrophages and LSECs, which indicated that antiviral molecules may have not been sufficiently 'sorted' by IFN-α-triggered hepatocytes.

Comparison of the abundance of exosomes in our study with their abundance under *in vivo* conditions is not feasible because the concentrations of exosomes and transfer efficiencies are probably different *in vitro* and *in vivo*. Nevertheless, we have provided various lines of evidence to support the proposal of a physiological role for exosomes in the IFN-α-induced antiviral response *in vivo*. First, the inhibition of exosome release by nSMase2- or Rab27a-specific shRNA significantly weakened both exogenous and endogenous IFN-α-induced antiviral activity *in vivo*. Second, after depletion of macrophages in mouse liver, a weaker antiviral response to HBV was induced by IFN-α in mice repopulated with BMDMs in which nSMase2 or Rab27a was knocked down than in mice repopulated with control BMDMs (with no knockdown). Finally, exosomes mediated transmission of the antiviral molecule APOBEC3G from adoptively transferred BMDMs to hepatocytes in the mouse liver after stimulation with IFN-α.

The manner by which treatment with IFN-α changed the profiles of exosomal molecules remains unclear. Our data indicated that the greater abundance of exosomal molecules did not necessarily result from higher expression in IFN-α-treated cells, consistent with the idea of the active 'sorting' or selective enrichment of RNA in exosomes[7–9]. A variety of studies have indicated that the 'sorting' of proteins into exosomes can depend on monoubiquitination, lipid or protein affinity, or higher order oligomerization[40]. However, the mechanisms that underlie the selective 'sorting' of mRNAs and miRNAs into exosomes are still poorly understood. We are tempted to hypothesize that when mRNA- or miRNA-binding proteins are 'sorted' into exosomes, those proteins carry the mRNA or miRNA into the exosomes as well. The components of miRNA effector complexes, such as AGO2 and its interacting partner GW182, have been shown to associate with MVBs and then be secreted by the exosomes[41], which perhaps indicates an exosome-specific miRNA-targeting mechanism. Further studies are needed to define the precise exosomal cargo-loading process and to understand how IFN-α exploits this process to promote or restrict the 'sorting' of cellular molecules into exosomes.

Although antiviral molecules can be conveyed by exosomes into cells in which HBV is replicating, the manner by which such molecules inhibit HBV replication remains largely unknown. Similar to our findings, one study has reported that APOBEC3G can be packaged and delivered to cells via exosomes to restrict replication of human immunodeficiency virus[42]. Although the anti-HBV effect of APOBEC3G is well established, there is no clear consensus on whether this activity is dependent on or independent of deaminase[43]. Overexpression of IFITM1 and GTPBP2 has also been shown to suppress HBV replication in hepatocyte-derived cells[44], and we have found that such inhibition may be due to blunted HBV promoter activity (data not shown). Moreover, TNFAIP8L2-deficient mice are reported to have more HBV replication than wild-type mice after hydrodynamic injection of an HBV-replicating plasmid, although the underlying mechanism is unclear[45]. The three miRNAs we studied here are less likely to directly target HBV RNA to restrict HBV propagation, as we found no predicted target sites for these three miRNAs in HBV transcripts by analysis of the miRBase searchable database of published miRNA sequences and annotation with TargetScan online software for the prediction of microRNA targets (data not shown). Clearly, the abundance of these antiviral molecules that resulted from transfection-based overexpression was far greater than the abundance that stemmed from exosome-mediated delivery. Thus, the exosome-mediated antiviral activity of IFN-α was probably due to a combination of all of the antiviral molecules.

Whether the exosome-mediated transfer of IFN-α-induced antiviral activity is a widespread mechanism adopted by hosts to control viral infection remains uncertain. In this study, we found that exosomes from IFN-α-treated macrophages and LSECs greatly restricted HCV replication. The inhibition of exosome release impaired the endogenous IFN-α-induced antiviral activity against MHV-A59 and adenovirus. In addition, several molecules transferred by the exosomes in our study have a broad antiviral spectrum. For example, IFITM1 has been shown to suppress the influenza A virus H1N1, West Nile virus, dengue virus, HCV and type 1 human immunodeficiency virus[46]. Notably, exosomes derived from macrophages, which are located in many tissues, were internalized by many types of cells, such as cells derived from the lung, kidney and uterus (data not shown). All of these observations seem to suggest that exosome-mediated transfer of IFN-α-induced antiviral activity is a common defense mechanism against invading viruses. Together, our results not only address the physiological role of exosomes in the IFN-α-induced antiviral response but also expand the fundamental understanding of the antiviral mechanism of IFN-α. Because of the side effects of IFN-α therapy and the limited responsiveness of patients to treatment with IFN-α, the delivery of powerful antiviral factors via exosomes may be a preferable therapeutic strategy that could lead to the development of new treatments for chronic infection with HBV and other infectious diseases.

METHODS

Methods and any associated references are available in the online version of the paper.

Accession codes. ArrayExpress: microarray data, E-MEXP-3900 and E-MEXP-3903.

Note: Supplementary information is available in the online version of the paper.

ACKNOWLEDGMENTS

We thank C. Dong, N. Weng, J. Guo, J. Hu, S. Zhou and Q. Cai for suggestions and critical reading of the manuscript. Supported by the National Key Basic Research Program of China (2012CB519000 to Z.Y.), the National Megaprojects of China for Infectious Diseases (2012ZX10002007-001 to Z.Y.), the German Research Foundation (SFB/Transregio TRR60 to Z.Y.), the National Natural Science Foundation of China (31200129 to J. Li) and the China Postdoctoral Science Foundation (201104232 to J. Li).

AUTHOR CONTRIBUTIONS

J. Li conceived of the study, designed the experiments, did most of the experiments and wrote the manuscript; K.L. isolated, characterized and labeled exosomes; Y.L. did quantitative RT-PCR; Y.X. and T.P. contributed to the HCV-replication assays; F.Z. generated the lentiviral expression vectors; H.Y. and X.Z. assisted in the hydrodynamic injections; J. Liu provided reagents; J.C. and M.W. helped with depletion and reconstitution of macrophages; and Z.Y. supervised all aspects of the study.

COMPETING FINANCIAL INTERESTS

The authors declare no competing financial interests.

1. Borden, E.C. *et al.* Interferons at age 50: past, current and future impact on biomedicine. *Nat. Rev. Drug Discov.* **6**, 975–990 (2007).
2. Chevaliez, S. & Pawlotsky, J.M. Interferons and their use in persistent viral infections. *Handb. Exp. Pharmacol.* **189**, 203–241 (2009).
3. Randall, R.E. & Goodbourn, S. Interferons and viruses: an interplay between induction, signalling, antiviral responses and virus countermeasures. *J. Gen. Virol.* **89**, 1–47 (2008).
4. Blalock, J.E. & Baron, S. Interferon-induced transfer of viral resistance between animal cells. *Nature* **269**, 422–425 (1977).
5. Théry, C., Ostrowski, M. & Segura, E. Membrane vesicles as conveyors of immune responses. *Nat. Rev. Immunol.* **9**, 581–593 (2009).
6. Mittelbrunn, M. & Sanchez-Madrid, F. Intercellular communication: diverse structures for exchange of genetic information. *Nat. Rev. Mol. Cell Biol.* **13**, 328–335 (2012).
7. Valadi, H. *et al.* Exosome-mediated transfer of mRNAs and microRNAs is a novel mechanism of genetic exchange between cells. *Nat. Cell Biol.* **9**, 654–659 (2007).
8. Skog, J. *et al.* Glioblastoma microvesicles transport RNA and proteins that promote tumour growth and provide diagnostic biomarkers. *Nat. Cell Biol.* **10**, 1470–1476 (2008).
9. Mittelbrunn, M. *et al.* Unidirectional transfer of microRNA-loaded exosomes from T cells to antigen-presenting cells. *Nat. Commun.* **2**, 282 (2011).
10. Montecalvo, A. *et al.* Mechanism of transfer of functional microRNAs between mouse dendritic cells via exosomes. *Blood* **119**, 756–766 (2012).
11. Meckes, D.G. Jr. *et al.* Human tumor virus utilizes exosomes for intercellular communication. *Proc. Natl. Acad. Sci. USA* **107**, 20370–20375 (2010).
12. Pegtel, D.M. *et al.* Functional delivery of viral miRNAs via exosomes. *Proc. Natl. Acad. Sci. USA* **107**, 6328–6333 (2010).
13. Mozes, L.W. Lack of interferon-induced transfer of viral resistance against murine leukemia virus or poliovirus in cocultivated cells. *Virology* **116**, 359–362 (1982).
14. Seeger, C. & Mason, W.S. Hepatitis B virus biology. *Microbiol. Mol. Biol. Rev.* **64**, 51–68 (2000).
15. Shepard, C.W., Simard, E.P., Finelli, L., Fiore, A.E. & Bell, B.P. Hepatitis B virus infection: epidemiology and vaccination. *Epidemiol. Rev.* **28**, 112–125 (2006).
16. Kwon, H. & Lok, A.S. Hepatitis B therapy. *Nat. Rev. Gastroenterol. Hepatol.* **8**, 275–284 (2011).
17. Li, J. *et al.* Inhibition of hepatitis B virus replication by MyD88 involves accelerated degradation of pregenomic RNA and nuclear retention of pre-S/S RNAs. *J. Virol.* **84**, 6387–6399 (2010).
18. Hiraga, N. *et al.* Absence of viral interference and different susceptibility to interferon between hepatitis B virus and hepatitis C virus in human hepatocyte chimeric mice. *J. Hepatol.* **51**, 1046–1054 (2009).
19. Lutgehetmann, M. *et al.* Hepatitis B virus limits response of human hepatocytes to interferon-α in chimeric mice. *Gastroenterology* **140**, 2074–2083 (2011).
20. Chen, J. *et al.* Hepatitis B virus polymerase impairs interferon-(-induced STA T activation through inhibition of importin-(5 and protein kinase C-δ. *Hepatology* **57**, 470–482 (2013).
21. Gao, B., Jeong, W.I. & Tian, Z. Liver: An organ with predominant innate immunity. *Hepatology* **47**, 729–736 (2008).
22. Ishibashi, H., Nakamura, M., Komori, A., Migita, K. & Shimoda, S. Liver architecture, cell function, and disease. *Semin. Immunopathol.* **31**, 399–409 (2009).
23. Wu, M. *et al.* Hepatitis B virus polymerase inhibits the interferon-inducible MyD88 promoter by blocking nuclear translocation of Stat1. *J. Gen. Virol.* **88**, 3260–3269 (2007).
24. Yang, P.L., Althage, A., Chung, J. & Chisari, F.V. Hydrodynamic injection of viral DNA: a mouse model of acute hepatitis B virus infection. *Proc. Natl. Acad. Sci. USA* **99**, 13825–13830 (2002).
25. Ke, B. *et al.* Adoptive transfer of ex vivo HO-1 modified bone marrow-derived macrophages prevents liver ischemia and reperfusion injury. *Mol. Ther.* **18**, 1019–1025 (2010).
26. Trajkovic, K. *et al.* Ceramide triggers budding of exosome vesicles into multivesicular endosomes. *Science* **319**, 1244–1247 (2008).
27. Kosaka, N. *et al.* Secretory mechanisms and intercellular transfer of microRNAs in living cells. *J. Biol. Chem.* **285**, 17442–17452 (2010).
28. Dreux, M. *et al.* Short-range exosomal transfer of viral RNA from infected cells to plasmacytoid dendritic cells triggers innate immunity. *Cell Host Microbe* **12**, 558–570 (2012).
29. Bianco, F. *et al.* Acid sphingomyelinase activity triggers microparticle release from glial cells. *EMBO J.* **28**, 1043–1054 (2009).
30. Zhang, J., Reedy, M.C., Hannun, Y.A. & Obeid, L.M. Inhibition of caspases inhibits the release of apoptotic bodies: Bcl-2 inhibits the initiation of formation of apoptotic bodies in chemotherapeutic agent-induced apoptosis. *J. Cell Biol.* **145**, 99–108 (1999).
31. Ostrowski, M. *et al.* Rab27a and Rab27b control different steps of the exosome secretion pathway. *Nat. Cell Biol* **12**, 19–30 (2010).
32. Thery, C., Amigorena, S., Raposo, G. & Clayton, A. in *Current Protocols Cell Biology* Ch 3, Unit 3, 22 (John Wiley & Sons, 2006).
33. Meckes, D.G. Jr. & Raab-Traub, N. Microvesicles and viral infection. *J. Virol.* **85**, 12844–12854 (2011).
34. Turelli, P., Mangeat, B., Jost, S., Vianin, S. & Trono, D. Inhibition of hepatitis B virus replication by APOBEC3G. *Science* **303**, 1829 (2004).
35. Park, I.H., Baek, K.W., Cho, E.Y. & Ahn, B.Y. PKR-dependent mechanisms of interferon-α for inhibiting hepatitis B virus replication. *Mol. Cells* **32**, 167–172 (2011).
36. Keller, S. *et al.* Systemic presence and tumor-growth promoting effect of ovarian carcinoma released exosomes. *Cancer Lett.* **278**, 73–81 (2009).
37. Weiss, S.R. & Navas-Martin, S. Coronavirus pathogenesis and the emerging pathogen severe acute respiratory syndrome coronavirus. *Microbiol. Mol. Biol. Rev.* **69**, 635–664 (2005).
38. DuPage, M., Dooley, A.L. & Jacks, T. Conditional mouse lung cancer models using adenoviral or lentiviral delivery of Cre recombinase. *Nat. Protoc.* **4**, 1064–1072 (2009).
39. Takahashi, K. *et al.* Plasmacytoid dendritic cells sense hepatitis C virus-infected cells, produce interferon, and inhibit infection. *Proc. Natl. Acad. Sci. USA* **107**, 7431–7436 (2010).
40. Record, M., Subra, C., Silvente-Poirot, S. & Poirot, M. Exosomes as intercellular signalosomes and pharmacological effectors. *Biochem. Pharmacol.* **81**, 1171–1182 (2011).
41. Gibbings, D.J., Ciaudo, C., Erhardt, M. & Voinnet, O. Multivesicular bodies associate with components of miRNA effector complexes and modulate miRNA activity. *Nat. Cell Biol.* **11**, 1143–1149 (2009).
42. Khatua, A.K., Taylor, H.E., Hildreth, J.E. & Popik, W. Exosomes packaging APOBEC3G confer human immunodeficiency virus resistance to recipient cells. *J. Virol.* **83**, 512–521 (2009).
43. Chang, J., Block, T.M. & Guo, J.T. The innate immune response to hepatitis B virus infection: implications for pathogenesis and therapy. *Antiviral Res.* **96**, 405–413 (2012).
44. Mao, R. *et al.* Indoleamine 2,3-dioxygenase mediates the antiviral effect of gamma interferon against hepatitis B virus in human hepatocyte-derived cells. *J. Virol.* **85**, 1048–1057 (2011).
45. Xi, W. *et al.* Roles of TIPE2 in hepatitis B virus-induced hepatic inflammation in humans and mice. *Mol. Immunol.* **48**, 1203–1208 (2011).
46. Diamond, M.S. & Farzan, M. The broad-spectrum antiviral functions of IFIT and IFITM proteins. *Nat. Rev. Immunol.* **13**, 46–57 (2013).

ONLINE METHODS

Plasmids, cells, Transwell coculture and transfection. The original pHBV1.3 HBV replicon construct[17] and pISRE-Luc construct[23] have been described. For construction of expression constructs for STAT1 and nSMase2 driven by the hepatocyte-specific promoter of the gene encoding albumin, cDNA encoding mouse STAT1 or nSMase2 was individually inserted into the pBluescript-ALB vector[47]. The promoter of the resultant expression plasmid for STAT1 or nSMase2 was replaced by the CMV promoter, a macrophage-specific promoter (of the gene encoding the receptor for macrophage colony-stimulating factor[48]) or an endothelial cell–specific promoter (of the gene encoding the tyrosine kinase receptor TIE-2)[49]. Expression constructs for exosomal mRNA (**Supplementary Table 2**) encoding proteins with carboxy-terminal Myc tags were from OriGene. For RNA-mediated interference, shRNA targeting the following molecules (National Center for Biotechnology Information Nucleotide database accession codes in parentheses) was constructed with the lentiviral vector pLKO.1 (Addgene): STAT1 (NM_007315 for human; NM_001205313 for mouse), nSMase2 (NM_018667 for human; NM_021491 for mouse), Rab27a (NM_004580 for human; NM_023635 for mouse), and APOBEC3G (NM_021822). For construction of the APOBEC3G-expressing lentiviral vector, the DNA fragment encoding eGFP-APOBEC3G carried on the pEGFP-C2 backbone (Clontech) was inserted into the pLJM1 vector (Addgene) under the control of the promoter of the gene encoding APOBEC3G. The siRNA-resistant cDNA of nSMase2 or Rab27a was inserted into the pLJM1 vector. Lentivirus was generated according to the manufacturer's instructions (Addgene). The mimics and inhibitors of the human miRNAs hsa-miR-638, hsa-miR-4284 and hsa-miR-1260 were from RuiboBio. Reporters containing three tandem repeats of artificial binding sites complementary to the seed sequences of the three miRNAs noted above were generated by cloning of those repeats into the pcDNA3.1-Luc vector[17]. Correct sequence of all constructs was confirmed by DNA sequencing.

HepG2.2.15 and HepG2 cells have been described[17]. The THP-1 cell line was from American Type Culture Collection. Human LSECs were from ScienCell. Cells were cultured at 37 °C in 5% CO_2 in RPMI-1640 medium containing 10% (vol/vol) FBS (FBS), 100 U/ml penicillin and 100 μg/ml streptomycin. The THP-1 cells were differentiated for 24 h by stimulation with 50 ng/ml PMA (phorbol 12-myristate 13-acetate; Sigma-Aldrich) to obtain a macrophage-like phenotype that closely resembled human monocyte–derived macrophages, as reported[50]. For coculture experiments, monocyte-derived macrophages or LSECs at a density of 2×10^5 cells per ml were cultured with HepG2.2.15 cells at a density of 8×10^5 cells per ml in a Transwell-6 system with a 0.4-μm porous membrane (Corning) to prevent both the transfer of vesicles larger than exosomes and direct cell contact. Cells were transfected according to the manufacturer's instructions with the transfection reagent FuGENE HP (Roche) or Lipofectamine 2000 (Invitrogen).

Immunoblot analysis. Immunoblot analyses were done with the appropriate antibodies (details, **Supplementary Table 3**) according to standard protocols[17,20].

Analysis of viral nucleic acid. HBV RNA was measured by RNA blot analysis with a ^{32}P-radiolabeled HBV DNA probe as described[17]. Intracellular HBV nucleocapsid–associated DNA and secreted HBV virions precipitated with 6% polyethylene glycol 8000 (PEG 8000) and anti-pre-S1 (sc-57761; SantaCruz), respectively, were analyzed by Southern blot as described[17].

For analysis of the deaminase activity of APOBEC3G, intracellular hypermutated HBV DNA was amplified by PCR at a low denaturation temperature of 88 °C, as reported[51]. This technique is based on the principle that DNA sequences with fewer interstrand hydrogen bonds dissociate more easily. If cytidine deamination occurs frequently, the resultant AT-rich viral DNA can be amplified at lower denaturation temperatures.

Exosome isolation, characterization, 'immunodepletion' and labeling. THP-1-derived macrophages and LSECs were grown in culture medium supplemented with 10% FBS (which was depleted of endogenous exosomes by overnight centrifugation at 100,000*g*) and were treated for 48 h with 1,000 U/ml IFN-α (PBL Interferon Source) or not. Exosomes from culture supernatants were isolated by differential centrifugation, as described[32], at 300*g* for 10 min, 2,000*g* for 10 min, 10,000*g* for 30 min and 100,000*g* for 70 min, followed by one wash with phosphate-buffered saline (PBS) and purification by centrifugation at 100,000*g* for 70 min. Purified exosomes were then characterized by electron microscopy, immunoblot analysis and sucrose-density-gradient centrifugation as described[32]. Protein concentrations of the exosome preparations were determined by the Bradford microassay method (Bio-Rad Laboratories).

For 'immunodepletion', cell culture supernatants were incubated overnight at 4 °C with biotinylated anti-CD63 (353017; Biolegend) or an isotype-matched (IgG) control antibody (400103; Biolegend), and immunocomplexes were captured by Streptavidin T1 beads (Invitrogen).

Purified exosomes were labeled with a PKH67 kit (Sigma) or SYTO RNASelect green fluorescent cell stain (Invitrogen) according to the manufacturer's instructions. HepG2.2.15 cells were incubated for 2 h at 37 °C with 5 μg/ml labeled exosomes. Where necessary, labeled exosomes were preincubated with 2 μg/ml annexin V (BD Biosciences). After cells were fixed, they were visualized with a confocal fluorescence microscope.

Microarray analysis. Exosomes from untreated or IFN-α-treated LSECs were isolated as described above. Microarray analysis of the exosomal mRNA and miRNA profiles was done by KangChen Bio-tech with the Agilent and Exiqon Array platforms, respectively, with three different exosome preparations.

Quantitative RT-PCR. A total of 50 fmol of synthetic *Caenorhabditis elegans* miRNA cel-miR-39 (RuiboBio) was added to each sample during the isolation of exosomal RNA. Quantitative RT-PCR was done in triplicate for each sample with SYBR-Green (Takara Bio). GAPDH was used for normalization of mRNA, and exogenous cel-miR-39 and endogenous U6 small nuclear RNA were used for normalization of exosomal and cellular miRNA, respectively. Data were analyzed by the change-in-cycling-threshold ($2^{-\Delta\Delta CT}$) method.

Hydrodynamic injection–mediated gene knockdown and 'rescue' in mouse liver. Approval for all of the experiments involving animals was obtained from the Institutional Animal Care and Use Committee at Fudan University. A total of 15 μg of pHBV1.3, together with 15 μg of the expression construct for shRNA targeting mouse STAT1 (or nSMase2 or Rab27a) or a control construct, was diluted in 2.0 ml saline and injected hydrodynamically into the tail vein of 6- to 8-week-old mice within 5–8 s as described[17], followed by treatment with mouse IFN-α (1.4×10^5 units per mouse) or saline 1 d after the hydrodynamic injection. Where necessary, a construct for the expression of mouse STAT1 (or nSMase2) was included in the transfection at a dose of 3 μg (for CMV promoter–driven expression) or 15 μg (for liver cell type–specific promoter–driven expression). Approximately 50 μl of serum was collected from the mice and treated overnight at 37 °C with 25 U of DNase I for analysis of viremia with a Qiagen PCR kit (Qiagen). Mouse single-liver-cell suspensions were prepared by two-step collagenase perfusion and filtration through a cell strainer with a pore size of 70-μm, followed by isolation of exosomes as described above. Where needed, the suspension was used for the isolation and purification of hepatocytes, macrophages and LSECs by Percoll density-gradient centrifugation and magnetic-activated cell sorting, as described[52]. The expression of STAT1 and nSMase2 in the total or specific mouse liver cells was assessed by immunoblot analysis.

***In vivo* adoptive transfer of *ex vivo*–modified BMDMs.** Mouse BMDMs were prepared by culture of bone marrow cells for 7 d in RPMI-1640 medium containing 10 ng/ml recombinant mouse macrophage colony-stimulating factor (R&D Systems). For experiments involving depletion of macrophages and reconstitution, mice were given intravenous injection of 200 μl of liposomal clodronate (Encapsula NanoSciences) for 48 h for depletion of macrophages in liver tissues. BMDMs infected with lentivirus expressing shRNA targeting STAT1 (or nSMase2 or Rab27a) or control shRNA were injected via the tail vein into the mice that had been depleted of macrophages (5×10^6 cells per mouse). Then, 24 h after cell administration, mice were given hydrodynamic injection of pHBV1.3 and treated for 48 h with 1.4×10^5 U of IFN-α. HBV DNA in the serum was measured as described above.

For confirmation of the exosome-mediated transfer of APOBEC3G *in vivo*, BMDMs were infected with a lentivirus expressing eGFP-APOBEC3G, driven

doi:10.1038/ni.2647

by the promoter of the gene enoding APOBEC3G alone or in combination with lentivirus expressing nSMase2-specific shRNA or control shRNA. Mice were injected with the modified BMDMs (5×10^6 cells per mouse), followed 24 h later by treatment for an additional 48 h with 1.4×10^5 units of IFN-α. Livers were thoroughly perfused with and fixed overnight at 4 °C in 4% paraformaldehyde. Nonspecific binding in liver tissue sections (10 μm in thickness) was blocked with 5% bovine serum albumin and sections were incubated with anti-GFP (G6539; Sigma) and anti-albumin (16475-1-AP; Proteintech) before confocal microscopy to locate eGFP-APOBEC3G. Mouse hepatocytes were isolated as described above for immunoblot analysis of eGFP-APOBEC3G.

***In vivo* viral infection model.** To inhibit exosome release in the mouse liver, 15 μg of the expression construct for mouse nSMase2-specific shRNA or a control construct was injected hydrodynamically into mice as described above. Then, 24 h later, mice were given injection of neutralizing antibody to IFN-α and IFN-β (22100-1 and 22400-1; PBL InterferonSource) or control antibody (sc-2026; Santa Cruz), followed by infection for an additional 48 h with MHV-A59 (5 plaque-forming units). Blood was collected for measurement of alanine aminotransferase, and liver and brain were weighed and homogenized and viral titers we measured by a standard plaque assay with L2 cells.

For inhibition of the release of exosomes in the mouse lung, lentivirus expressing mouse nSMase2–specific shRNA was delivered into the mouse lung (1×10^6 viruses per mouse) by intranasal inhalation according to a published protocol[38]. At 24 h after the intranasal infection, mice were given injected with IFN-α/β-neutralizing antibody or control antibody, followed by intranasal infection for an additional 72 h with recombinant adenovirus encoding GFP (1×10^9 plaque-forming units). Total genomic DNA was isolated from liver and copies of adenovirus genome were measured by quantitative real-time PCR.

Statistics. Statistical comparisons were made by ANOVA or a two-tailed Student's *t*-test; *P* values of 0.05 or less were considered statistically significant.

47. Pinkert, C.A., Ornitz, D.M., Brinster, R.L. & Palmiter, R.D. An albumin enhancer located 10 kb upstream functions along with its promoter to direct efficient, liver-specific expression in transgenic mice. *Genes Dev.* **1**, 268–276 (1987).
48. Zhang, D.E., Hetherington, C.J., Chen, H.M. & Tenen, D.G. The macrophage transcription factor PU.1 directs tissue-specific expression of the macrophage colony-stimulating factor receptor. *Mol. Cell. Biol.* **14**, 373–381 (1994).
49. Fadel, B.M., Boutet, S.C. & Quertermous, T. Octamer-dependent *in vivo* expression of the endothelial cell-specific TIE2 gene. *J. Biol. Chem.* **274**, 20376–20383 (1999).
50. Auwerx, J. The Human leukemia-cell line, Thp-1—a multifaceted model for the study of monocyte-macrophage differentiation. *Experientia* **47**, 22–31 (1991).
51. Köck, J. & Blum, H.E. Hypermutation of hepatitis B virus genomes by APOBEC3G, APOBEC3C and APOBEC3H. *J. Gen. Virol.* **89**, 1184–1191 (2008).
52. Liu, W. *et al.* Sample preparation method for isolation of single-cell types from mouse liver for proteomic studies. *Proteomics* **11**, 3556–3564 (2011).